Medicinal Chemistry Research
https://doi.org/10.1007/s00044-020-02667-5

MEDICINAL CHEMISTRY RESEARCH

ORIGINAL RESEARCH

Antioxidant and acetylcholinesterase inhibition activity of aliphatic and aromatic edaravone derivatives

Victor Wagner Barajas-Carrillo[1] · Arturo Estolano-Cobián[1] · Laura Díaz-Rubio[1] · Rocío Rosario Ayllón-Gutiérrez[1] · Ricardo Salazar-Aranda[2] · Raúl Díaz-Molina[3] · Víctor García-González[3] · Horacio Almanza-Reyes[4] · Ignacio A. Rivero[5] · Joaquín G. Marrero[6] · Iván Córdova-Guerrero[1]

Received: 16 September 2020 / Accepted: 5 November 2020

Abstract

As Alzheimer disease (AD) is a multifactorial condition, it should be tackled with drugs targeting multiple key pathways. A series of aliphatic (**2**–**8**) and aromatic (**9**–**15**) edaravone derivatives were synthesized, characterized, and evaluated as antioxidant agents using 1,1-diphenyl-2-picrylhydrazyl (DPPH) and 2-2'-azino-bis-(3-ethylbenzothiazoline-6-sulfonate) ($ABTS^{\cdot+}$) assays, as well as acetylcholinesterase (AChE) inhibitors. In both antioxidant assays, even though the starting compound edaravone was more active, the best derivative was **5** with 50% effective concentration (EC_{50}) of 0.0301 and 0.8106 mM respectively, followed by **3** (EC_{50} of 0.1920 mM and 3.5311 mM). In the AChE inhibition assay, the derivatives were not as active as the positive control galantamine, but a general better activity was shown from the aromatic compounds. The best results were for **10**, with 41.9% of inhibition (concentration of 150 µg/mL), and **9** with 31.6%. Docking analysis of compound **10** showed hydrogen bonds with residues Ser200 and His440 in the AChE catalytic gorge. All synthesized derivatives **2**–**15** presented drug-like properties and are capable of crossing the blood–brain barrier and not be pumped out of it. These results indicate edaravone derivatives can function as scaffolds for AD drugs, though further derivatizations should be conducted to improve their antioxidant and AChE inhibition profiles.

Graphical Abstract

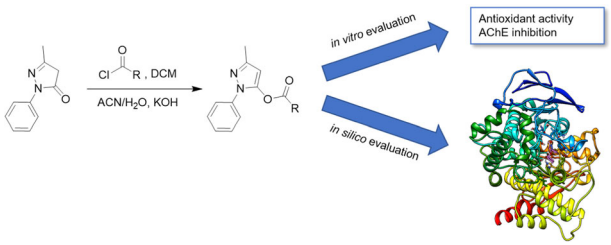

Supplementary information The online version of this article (https://doi.org/10.1007/s00044-020-02667-5) contains supplementary material, which is available to authorized users.

✉ Iván Córdova-Guerrero
icordova@uabc.edu.mx

[1] Facultad de Ciencias Químicas e Ingeniería, Universidad Autónoma de Baja California, 22390 Tijuana, B.C., Mexico

[2] Departamento de Química Analítica, Facultad de Medicina, Universidad Autónoma de Nuevo León, San Nicolás de los Garza, 64460 Monterrey, Mexico

[3] Departamento de Bioquímica, Facultad de Medicina Mexicali, Universidad Autónoma de Baja California, 21000 Mexicali, Mexico

[4] Facultad de Medicina y Psicología, Universidad Autónoma de Baja California, 22390 Tijuana, B.C., Mexico

[5] Centro de Graduados e Investigación en Química, Tecnológico Nacional de México/Instituto Tecnológico de Tijuana, 22510 Tijuana, B.C., Mexico

[6] Instituto Politécnico Nacional, UPIIG, Silao de la Victoria, Guanajuato, Mexico

Published online: 23 November 2020

Keywords Edaravone · Antioxidant · Acetylcholinesterase inhibition · Docking · ADME calculation

Introduction

The neurodegenerative disorder Alzheimer's disease (AD) is the main cause of dementia in elderly patients [1], AD being characterized by global cognitive impairment, including progressive memory loss and declined reasoning [2, 3]. Several pathogenic mechanisms have been suggested in the development of AD. Currently, therapeutic interventions target these proposed mechanisms, namely, the antioxidant therapy against oxidative stress caused by free radicals and the inhibition of acetylcholinesterase (AChE) to compensate the loss of cholinergic function [4].

The aging process diminishes the free radical-scavenging ability by endogenous mechanisms [5]. Free radicals are nocent agents able to cause irreversible oxidative damage to cellular constituents [6]; under normal physiological conditions, the organism exhibits a variety of antioxidant mechanisms to counterbalance the potential damage of oxidants [7]. When the balance between free radicals and antioxidants is disrupted, it leads to a state known as oxidative stress [8], which translates into several pathologies, including cancer, hypertension, diabetes, and neurological disorders, including AD [9].

The brain contains an abundance of highly oxidizable polyunsaturated fatty acids and a high demand for oxygen [10], hence its vulnerability to damage caused by oxidant agents. In patients with AD, the brain displays higher levels of lipid peroxidation products and increased carbonyls derived from protein oxidation in neuronal cytoplasm; these abnormalities provide evidence of the connection between oxidative stress with this neurodegenerative disorder [11, 12].

AD progression is also related to another pivotal mechanism: cholinergic dysfunction [13], which states that deficiency of crucial neurotransmitter acetylcholine (ACh) in the brain of people with AD is due to insufficient production of ACh or the augmented activity of enzyme AChE [14], leading to the loss of cognitive capacity and general motor skills [15]. Common treatment for AD relies on drugs that increase concentration of ACh neurotransmitter by inhibiting AChE activity, with donepezil, galantamine, and tacrine, being the most used drugs [16]. Although well tolerated, AChE inhibitors (AChEIs) cause characteristic side effects, including nausea, dizziness, and sleep disturbances [17].

Pyrazolone and its derivatives are a pharmacological important group of compounds; these five-membered heterocyclic lactam rings display a wide range of biological activities, such as antipyretic, analgesic, anti-inflammatory, antitumor, and antioxidant activities [18, 19]. Edaravone is a pyrazolone, structure of which can be seen in Fig. 1, along with a series of related structures such as phenidone, a dual cyclooxygenase COX-2 and lipoxygenase 5-LOX inhibitor with chemopreventive profile [20], and dipyrone, a widely used analgesic, from which recently it has been reported that one of its metabolites can act as a cannabinoid receptor 1 agonist [21]; these are some examples that show the importance of the pyrazolone-like moieties in biological studies.

Edaravone is a free radical scavenger and nootropic, and its derivatives have been reported to exhibit diverse medicinal activities, including antitumoral, antiviral, and protective effect against sleep deprivation-related memory impairment [22–26].

Edaravone, which can also be found by the names methylphenylpyrazolone or norphenazone, to name a couple, has demonstrated different bioactivities, such as reduction of inflammation and oxidative stress response in acute cerebral infarction patients, in the treatment of injury in acute pancreatitis, in the treatment in craniocerebral injury, prevention of ferroptosis in amyotrophic lateral sclerosis (ALS) patients, and in asthma treatment through anti-inflammatory and antioxidative effects [27–31]. Furthermore, its use with the commercial name Radicava for the treatment of ALS by the Food and Drug Administration in USA has been approved [30]. Several of these above-mentioned edaravone properties point out to its antioxidant

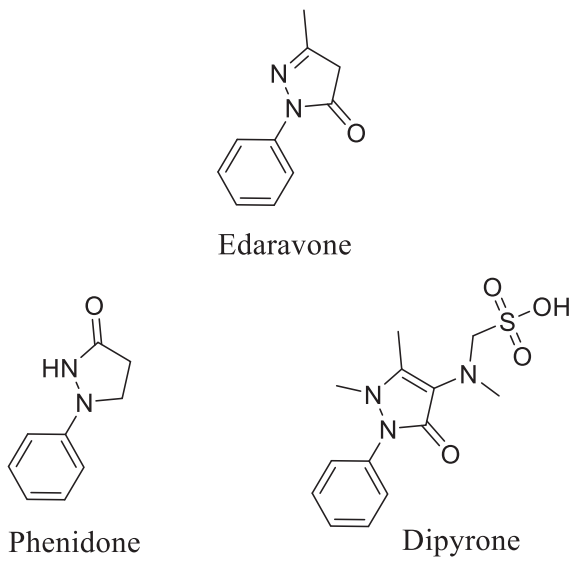

Fig. 1 Edaravone and related compounds structures

capabilities; therefore, it should be an interesting scaffold to start our search for antioxidant and AChEIs.

The aim of this study is to design and synthesize edaravone derivatives, incorporating in the pyrazolone ring different acyl fragments with aliphatic and aromatic substitutions, and evaluate in vitro their antioxidant capacity and AChE inhibition activity. In addition, in silico determinations were conducted, as docking for the exploration of AChE inhibition results, and the calculation of the drug-like properties of the synthesized compounds.

Results and discussion

Synthesis

The synthetic procedure employed was based on previous works of 4-substituted edaravone derivatives [32, 33] with some modifications. Reaction between the starting material edaravone **1** with different alkyl and aryl chlorides was performed in order to get the 4-substituted compounds. The main product of each reaction, as seen from the yields obtained (70–99%), was purified and characterized. However, no incorporation was detected in position 4 of edaravone. Instead, the spectroscopic data shows the incorporation of the new fragments as ester groups. Ester derivatives from edaravone after the synthesis by Jensen [32] have been reported before as side products from the synthetic procedure, although they can also be synthesized as the main one [34]. This could be due to the initial basic conditions, which are intended to remove the acidic hydrogen in position 4, so that this position can react with the alkyl and aryl chlorides. After the hydrogen removal, the pyrazolone ring could rearrange to an enolate form, where the oxygen would be reacting with the alkyl chlorides, generating the products **2**–**15**, as seen in Scheme 1. The substitutions in the incorporated carbonyl show aliphatic chains with varying lengths (**2**–**8**), as well as aromatic rings adjacent or separated (**9**–**15**) from the incorporated carbonyl. The proposed structures were analyzed and confirmed through infrared (IR) spectroscopy and mass spectroscopy (MS) and with ^{1}H- and ^{13}C-nuclear magnetic resonance (NMR).

In IR spectroscopy, the synthesized compounds showed bands for their aromatic C-H bonds between 3023 and 3069 cm^{-1}, as even the aliphatic derivatives have an aromatic ring in their core. For the incorporated fragments, the carbonyl band appears between 1709 and 1784 cm^{-1} for the C=O bond. The expected shifts and multiplicities were observed for the ^{1}H- and ^{13}C-NMR signals. For the common core structure, the aromatic hydrogens were present at $\delta = 7.62–7.16$, with the methyl in position 7 at $\delta =$ 2.40–2.28 and the singlet for one hydrogen in position 4 at $\delta = 6.26–6.07$, in accordance with the reference for the edaravone ester derivatives [34]. In ^{13}C-NMR, along with the new signals for the appropriate aliphatic or aromatic carbons, the carbon position 14 in the appropriate range $\delta =$ 172.4–161.9 for ester carbonyls of compounds **2**–**12**, **14**, and **15**, with a $\delta = 149.7$ for compound **13** as the incorporated carbonyl is a carbamate one, can be highlighted.

From the synthesized compounds, **2** [35], **6**, **7** [36], **9** [37], **10** [38], **11** [37], and **14** [39], there are previous reports of their synthesis. However, to the best of our knowledge products **3**, **4**, **5**, **8**, **12**, **13**, and **15** are reported for the first time in this work.

Antioxidant evaluation

Previous antioxidant evaluations of edaravone derivatives and analogs, both in in vitro assays and computational analysis [40, 41], point out the single electron transfer and hydrogen atom transfer as the proposed mechanisms for the antioxidant properties of these compounds [42]. For the electron transfer mechanism, this depends on the electron density of the pyrazolone ring of edaravone [43]. In the case of the hydrogen atom transfer mechanism, such as the 1,1-diphenyl-2-picrylhydrazyl (DPPH) assay, edaravone scavenges DPPH by donation of the H atom at position 4 [40].

By employing acyl chlorides as reacting agents in the incorporation of fragments in the pyrazolone ring, the synthesized products have an ester or carbamate (compound **13**) carbonyl attached to the before-mentioned ring. These groups with alkyl and aryl variations incorporated in these fragments were proposed to further explore the modulation of the antioxidant activity of edaravone derivatives, which was measured with the DPPH and 2-2'-azino-bis-(3-ethylbenzothiazoline-6-sulfonate) ($ABTS^{\cdot+}$) assays.

As stated in the methodology section, the synthesized compounds were prepared and evaluated in serial dilutions, their EC_{50} in mg/mL can be seen in Table 1, and in order to compare the products accounting their different molecular weights, their EC_{50} is also reported as mM. In the DPPH assay, the positive control quercetin showed the best antioxidant activity with an EC_{50} of 0.0028 mM, being followed by **1** with 0.0180 mM, and the derivatives showed lower antioxidant activity compared to edaravone. However, through the DPPH assay compounds **1**–**15** presented better antioxidant properties, compared with the results obtained from the $ABTS^{\cdot+}$ evaluation.

Following **1**, the better result for a derivative was for compound **5**, with an EC_{50} of 0.0301 mM. Product **12** and **3** were the next most active derivatives, with EC_{50} of 0.1603 and 0.1920 mM, respectively. Both **5** and **3** have aliphatic non-branched R fragments with four and two carbon atoms (Scheme 1), while **12** is from the aromatic derivatives and

Scheme 1 Synthesis of edaravone derivatives **2–15**

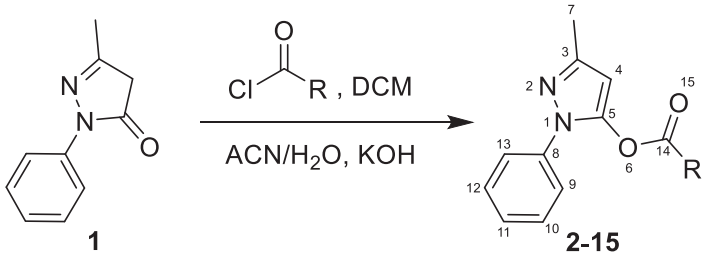

Compound	R	Compound	R
2		**9**	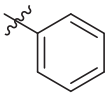
3		**10**	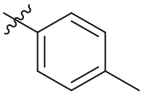
4		**11**	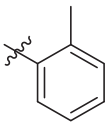
5	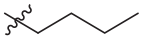	**12**	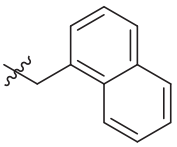
6	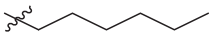	**13**	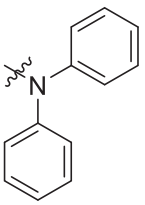
7	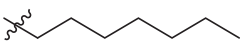	**14**	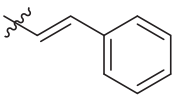
8	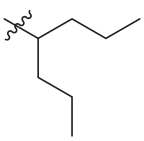	**15**	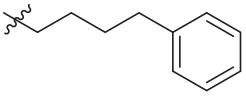

Table 1 Percentage of antioxidant activity of compounds **1**–**15**

Compound	DPPH		ABTS	
	EC_{50} (mg/mL)	EC_{50} (mM)	EC_{50} (mg/mL)	EC_{50} (mM)
1	0.0031 ± 0.001	0.0180	0.0357 ± 0.042	0.2049
2	0.3704 ± 0.243	1.7127	1.0660 ± 0.658	4.9297
3	0.0442 ± 0.073	0.1920	0.8131 ± 0.499	3.5311
4	1.1367 ± 0.156	4.6531	4.6446 ± 0.807	19.0126
5	0.0078 ± 0.017	0.0301	0.2094 ± 0.866	0.8106
6	0.3966 ± 0.309	1.3849	1.5406 ± 0.082	5.3796
7	1.0867 ± 0.101	3.6175	28.765 ± 0.34	95.7557
8	7.4140 ± 0.953	24.6804	31.245 ± 2.08	104.0113
9	1.3101 ± 0.272	4.7074	3.9011 ± 0.072	14.0171
10	0.5135 ± 0.063	1.7563	9.5909 ± 0.831	32.8073
11	0.4504 ± 0.108	1.5408	6.0331 ± 0.594	20.6373
12	0.0549 ± 0.053	0.1603	1.2631 ± 0.133	3.6890
13	ND	—	ND	—
14	0.4220 ± 0.030	1.3866	6.7344 ± 0.820	22.1272
15	0.5522 ± 0.824	1.6512	12.247 ± 0.20	36.6216
[a]**Quercetin**	0.0008 ± 0.037	0.0028	0.075 ± 0.002	0.2482

Values are mean ± SD, $n = 3$

ND not determined

[a]Served as reference compound

the only one with two aromatic rings (as **13** could not be evaluated due to poor solubility in the antioxidant assays).

In the $ABTS^{\cdot+}$ antioxidant evaluation, although this radical can be neutralized through different mechanisms, including also hydrogen transfers [44], in this assay the results were less active compared with the DPPH assay. The positive control presented an EC_{50} of 0.2482 mM, and **1** showed 0.2049 mM. As in the DPPH analysis, the derivatives were not as active as edaravone; nevertheless, in both techniques the better antioxidant derivative was **5**, as in the $ABTS^{\cdot+}$ assay it showed an EC_{50} of 0.8106 mM. It also concurs that the following more active products are **3** (3.5311 mM) and **12** (3.6890 mM). In each of the antioxidant assays, the less active product was **8**, with EC_{50} of 24.6804 and 104.0113 mM in DPPH and the $ABTS^{\cdot+}$ assays, respectively. As **8** presented such a low activity, and **4** was not as active as **5** and **3**, it could be possible that in the aliphatic derivatives the antioxidant activity is enhanced by short and non-branched chains adjacent to the incorporated carbonyl.

AChE inhibitory activity

Edaravone has been related to AD treatment through different mechanisms, mainly by reduction of amyloid-β (Aβ) peptide deposition, disaggregation of Aβ fibrils, oxidative stress diminution, attenuating tau hyperphosphorylation, and neuroinflammation, among other mechanisms [45, 46]. It has been reported that edaravone could inhibit AChE in rats injected with Aβ [47]; however, in a study with cisplatin-treated rats, edaravone inhibited the AChE levels that were increased by concomitant cisplatin treatment, but edaravone alone did not alter AChE levels [48]. As AD has been cataloged as a multifactorial disease and currently there is no effective drug for it, the suggested therapeutic approach is to target multiple key pathways [45]. Therefore, we searched for the synthesized edaravone derivatives both to display antioxidant properties and to act as AChEIs.

The results from the AChE inhibition assay can be seen in Table 2, where the positive control galantamine presented the highest inhibition percentage (91.9%). Edaravone percentage could not be determined due to the sample color interference in the analysis. As for the synthesized derivatives, the most active were **10** and **9**, with 41.9 and 31.6% of inhibition, respectively. These two products share as characteristic an aromatic ring adjacent to the ester carbonyl in the incorporated fragments. The other compound that shares this structure is **11**, being a position isomer of **9**; therefore, the *ortho* position of the methyl substitution in the aromatic ring of **11** could be responsible for the decrease in the activity, as this product only presented 16.3%. This result is in agreement with the literature, where in some families of compounds the *ortho* substitutions tend to be less active than the *para* substitutions [49–51].

From the aliphatic derivatives, compounds **6**, **4**, **8**, and **7** were the less active products (4.8, 3.0, 2.0, and 1.7%, respectively), so in a similar way to the aliphatic antioxidant results, a short and linear chain tend to be better for the

Table 2 Acetylcholinesterase inhibition of compounds **1–15**

Compound	% inhibition (150 µg/mL)
1	ND
2	20.7 ± 4.9
3	25.8 ± 7.4
4	3.0 ± 1.0
5	28.9 ± 8.6
6	4.8 ± 1.0
7	1.7 ± 0.8
8	2.0 ± 1.2
9	31.6 ± 8.1
10	41.9 ± 7.3
11	16.3 ± 3.3
12	16.9 ± 1.8
13	23.9 ± 2.8
14	19.5 ± 4.7
15	2.8 ± 1.8
[a]**Galantamine**	91.9 ± 0.82

Values are mean ± SD, $n = 3$

ND not determined

[a]Served as reference compound

AChE inhibition activity. In the case of the aromatic derivatives **9–15**, it can be highlighted that, in general, the aromatic compounds were better inhibitors compared to the aliphatic ones. The exception to this observation is product **15**, which was almost inactive with 2.8% of inhibition. This could be explained as for the derivative that shows with its aromatic ring a larger chain separation to the incorporated ester carbonyl, and as discussed with the aliphatic derivatives, the long aliphatic chain appears to diminish the AChE inhibition activity.

Molecular docking

In order to further explore the results obtained in vitro in the AChE inhibition assay, the most active synthesized derivative **10** was evaluated in silico through its docking against AChE. The enzyme molecular structure was selected from the Protein Data Bank (PDB ID: 1EVE), corresponding to the AChE from *Tetronarce californica* (*Tc*AChE), which shows a high similarity to the human one and therefore can be employed for the docking analysis [52]. As galantamine was employed as positive control in the in vitro assay, it was also docked against the *Tc*AChE model, as well the enzyme co-crystallized ligand donepezil.

The docking results can be seen in Table 3, where a more negative docking score represents a better ligand–receptor affinity. Galantamine, as a positive control in the in vitro assay, presented the best AChE inhibition percentage (91.9%), although in the docking analysis its score of

Table 3 Docking scores of **10** and reference compounds with AChE (PDB ID: 1EVE)

Compound	Binding energy (kcal/mol)	Principal residue interactions
10	−9.70	Phe331, Ser200, His440
[a]**Donepezil**	−11.2	Trp84, Trp279
[a]**Galantamine**	−9.26	Trp84, Ser200, His440, Glu199

[a]Served as reference compound

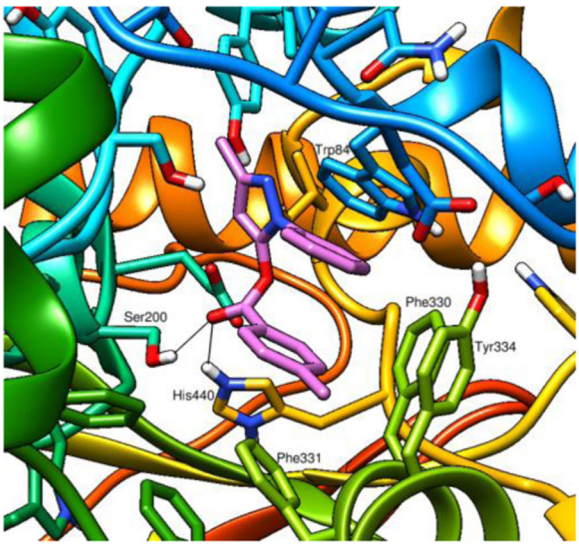

Fig. 2 Docking pose and interactions of compound **10** (purple) with the catalytic gorge of *Tc*AChE. Hydrogen bonds are represented by black lines

−9.26 kcal/mol was slightly higher than derivative **10**, which showed −9.70 kcal/mol. The in vitro result could be explained nevertheless as the docked pose is very similar to the crystallographic one obtained by [53], where galantamine shows hydrogen bonds with Ser200 and His440, two of the catalytic enzyme residues, and with Glu199. Compound **10** shows the first two interactions but lack the bond with Glu199. In the case of donepezil, as the co-crystallized ligand for the *Tc*AChE model, it scored accordingly the best docking result with −11.2 kcal/mol.

The synthesized compound **10** was the most active edaravone derivative in vitro with 41.9% inhibition. In the docking analysis, it showed a score of −9.70 kcal/mol, and its resulting docked pose in the *Tc*AChE catalytic gorge present the residues that could interact with them by hydrogen bonds and hydrophobic and π–π interactions (Fig. 2). The oxygen in the carbonyl behaves as the hydrogen bond acceptor for these before-mentioned interactions. Additionally, compound **10** shows its *p*-methyl benzyl ring in the vicinity of hydrophobic residues Phe330 and Phe331, where a π–π interaction is almost established

with Phe331; however, it is very clear that an intramolecular π–π interaction found as the benzyl ring in the core of **10** is completely overlapped with the incorporated *p*-methyl benzyl ring.

ADME (Absorbed, Distributed, Metabolized, or Eliminated) calculations

In Table 4 can be seen the predicted pharmacokinetics and drug-like properties of the compounds **1**–**15**, as predicted from the SwissADME server. Having Lipinski's rule [54] as a good guideline for the drug-like properties of new compounds (considering descriptors such as H bonds donors and acceptors, molecular weight, and lipophilicity), only products **12**, **13**, and **15** show one Lipinski's rule violation, having an MLogP >4.15. The rest of the synthesized compounds comply fully to these guidelines, presenting drug-like properties. Furthermore, all compounds show a high predicted gastrointestinal absorption.

Regarding the aim of the synthesized molecules as AChEI (and potentially leading to AD treatment), it is important for them to be capable to cross the blood–brain barrier (BBB), which is usually related to small and lipophilic molecules, of <400–500 Da [55]. As shown in Table 4, the molecular weight of compounds **1**–**15** fulfill this requirement, and all their Log *P* (1.64–4.46) show a more lipophilic character over a hydrophilic one. The SwissADME server predicts that all our compounds are BBB permeant, which could help in future in vivo studies in Alzheimer's treatment due to this activity. Moreover, the results show that all the products are not substrate for the permeability glycoprotein (P-gp). As this protein works by pumping out xenobiotics of the central nervous system (CNS), and therefore could interfere with AD treatment [55], the predicted properties of the synthesized compounds suggest that they can work as scaffolds for further developing new and better AD drugs.

Conclusion

In the search for new AD treatments, this work proposes the derivatization of edaravone, in order to obtain products that can possess different pharmacological mechanisms to improve their profile as potential AD drugs. Reacting edaravone with different aliphatic and aromatic acyl halides, a family of compounds were synthesized, characterized, and evaluated as antioxidants and AChEIs.

Compounds **1**–**15** showed through ADME calculations to have desirable drug-like properties, highlighting their capacity to cross the BBB and not to be pumped out by the P-gp, which could facilitate them to exert their activities in the CNS. This points out that edaravone derivatives with

Table 4 Pharmacokinetics and drug-likeness of compounds **1**–**15**, calculated by SwissADME

Descriptor	Molecule														
	1	2	3	4	5	6	7	8	9	10	11	12	13	14	15
MW	174.2	216.24	230.26	244.29	258.32	286.37	300.4	300.4	278.31	292.33	292.33	342.39	369.42	304.34	334.41
#H-bond acceptors	2	3	3	3	3	3	3	3	3	3	3	3	3	3	3
#H-bond donors	0	0	0	0	0	0	0	0	0	0	0	0	0	0	0
TPSA	32.67	44.12	44.12	44.12	44.12	44.12	44.12	44.12	44.12	44.12	44.12	44.12	47.36	44.12	44.12
MLOGP	1.6	2.28	2.55	2.82	3.07	3.56	3.8	3.8	3.6	3.84	3.84	4.29	4.59	3.73	4.25
Consensus Log P	1.64	2.21	2.53	2.86	3.23	3.95	4.32	4.16	3.39	3.72	3.67	4.34	4.46	3.72	4.36
Log S (Ali)	−1.56	−2.95	−3.44	−4.03	−4.37	−5.49	−6.05	−5.89	−4.67	−5.04	−5.04	−5.89	−6.25	−5.11	−5.84
Ali class	Very soluble	Soluble	Soluble	Moderately soluble	Moderately soluble	Moderately soluble	Poorly soluble	Moderately soluble	Moderately soluble	Moderately soluble	Moderately soluble	Moderately soluble	Poorly soluble	Moderately soluble	Moderately soluble
GI absorption	High	High	High	High	High	High	High	High	High	High	High	High	High	High	High
BBB permeant	Yes	Yes	Yes	Yes	Yes	Yes	Yes	Yes	Yes	Yes	Yes	Yes	Yes	Yes	Yes
P-gp substrate	No	No	No	No	No	No	No	No	No	No	No	No	No	No	No
CYP1A2 inhibitor	Yes	Yes	Yes	Yes	Yes	Yes	Yes	Yes	Yes	Yes	Yes	Yes	Yes	Yes	Yes
CYP2C19 inhibitor	No	Yes	Yes	Yes	Yes	Yes	Yes	Yes	Yes	Yes	Yes	Yes	Yes	Yes	Yes
CYP2C9 inhibitor	No	No	No	Yes	Yes	Yes	Yes	Yes	Yes	Yes	Yes	Yes	Yes	Yes	Yes
CYP2D6 inhibitor	No	No	No	No	No	No	No	No	No	No	No	No	No	No	No
CYP3A4 inhibitor	No	No	No	No	No	No	No	No	No	No	No	No	No	No	No
Lipinski #violations	0	0	0	0	0	0	0	0	0	0	0	1	1	0	1

MW molecular weight, *TPSA* topological polar surface area, Log P logarithm of the partition coefficient, *Log S (Ali)* Ali et al. [67] model logarithm of molar solubility in water, *GI* gastrointestinal, *BBB* blood–brain barrier, *P-gp* permeability glycoprotein, *CYP* cytochrome

aliphatic and aromatic esters in the pyrazol ring can be a good scaffold in the search of new AD drugs.

Preliminarily, the antioxidant results indicate that in the aliphatic derivatives the antioxidant activity is improved by short and non-branched chains, although further explorations are suggested to improve the current antioxidant profiles. The AChE inhibition of the synthesized derivatives again points out to short linear fragment derivatives as more active compounds compared to the ones with longer aliphatic chains. However, the enzyme inhibition was improved with the aromatic derivatives, especially when the aromatic ring was adjacent to the incorporated ester carbonyl (compounds **10** and **9**). Docking analysis of **10** suggest that this could be due to hydrogen bonds, with hydrophobic and π–π interactions in the enzyme catalytic gorge with the incorporated aromatic ring. As the products synthesized in this work were mainly hydrocarbon ones, further derivatizations with heteroatom groups are proposed to be incorporated, especially in the aromatic derivatives, to further improve their antioxidant and AChE inhibition activities.

Experimental/material and methods

Chemistry

All commercial reagents and solvents were purchased and used without previous purification. The synthesized products were purified through column chromatography with silica gel 60 Å, 230–400 mesh (Sigma-Aldrich). Purity of the products was first monitored by thin-layer chromatography (TLC) carried out in aluminum backed silica plates (Merck) revealed by ultraviolet (UV) light at 254 nm. For the chemical characterization of the synthesized products, melting points were taken on a Mel-Temp melting point apparatus (Thermo Scientific). Gas chromatography–MS was performed on a TRACE 1310 chromatograph and single quadrupole ISQ LT mass spectrometer (both from Thermo Scientific). Fourier-transform IR spectroscopy was performed on a Thermo Scientific Nicolet iS 5 spectrometer. NMR spectra were obtained on a 400 MHz Avance DPX spectrometer (Bruker). The chemical shifts in NMR spectra (δ) are presented with tetramethylsilane as the internal standard (δ: 0.00). Chemical shifts are given in ppm, coupling constants J are expressed in Hertz (Hz) (multiplicity: s = singlet, d = doublet, dd = doublet of doublet, ddd = doublet of doublet of doublet, t = triplet, tt = triplet of triplet, q = quadruplet, quint = quintuplet, sext = sextuplet, sept = septuplet, m = multiplet). UV–visible spectra for the antioxidant assays were obtained on a Genesys 20 (Thermo Scientific) spectrophotometer, while a Microplate reader Multiskan FC was employed for the AChE assay.

Synthesis of edaravone derivatives

In a round bottom flask, 5 Eq of KOH were dissolved in an acetonitrile and water mixture under magnetic stirring. After complete dissolution, 1 Eq of edaravone (**1**) was added, and the mixture was left under strong stirring for 30 min. Subsequently, 2 Eq of the corresponding acyl halide dissolved in dichloromethane (DCM) was transferred to the reaction and the stirring continued for 5 min (Scheme 1). Afterwards, the reaction mixture was washed with a saturated sodium bicarbonate solution, and the product was extracted with DCM. The reactions were monitored by TLC and the products were purified by column chromatography. The structures of the products were confirmed by MS and NMR spectra as discussed below and in Supplementary Figs. S1–S28.

3-methyl-1-phenyl-1*H*-pyrazol-5-yl acetate (2)

Brownish-orange viscous oil (yield 97%); $C_{12}H_{12}N_2O_2$; IR (attenuated total reflection (ATR) diamond, cm^{-1}) 3063 (C-H aromatic), 2961 (C-H aliphatic), 1706 (C=O), 1498 (C-C) cm^{-1}; ^{1}H NMR ($CDCl_3$, 400 MHz,): $\delta = 7.55–7.51$ (2H, m, H-13, H-9), 7.46–7.41 (2H, m, H-12, H-10), 7.34–7.29 (1H, m, H-11) 6.09 (1H, s, H-4), 2.32 (3H, s, H-7), 2.25 (3H, s, H-16); ^{13}C NMR ($CDCl_3$, 100 MHz): $\delta = 166.1$ (C, C-14), 148.9 (C, C-3), 144.3 (C, C-5), 138.1 (C, C-8), 129.1 (CH, C-12, C-10), 127.1 (CH, C-11), 123.0 (CH, C-13, C-9), 95.9 (CH, C-4), 20.8 (CH_3, C-16), 14.5 (CH_3, C-7); electron ionization MS (EIMS) *m/z* (rel. int.) 216 $[M]^+$ (1), 174(23), 129(5), 91(2), 77(41), 68(5), 51(28), 43(100).

3-methyl-1-phenyl-1*H*-pyrazol-5-yl propionate (3)

Dark orange viscous oil (yield 99%); $C_{13}H_{14}N_2O_2$; IR (ATR diamond, cm^{-1}) 3069 (C-H aromatic), 2928 (C-H aliphatic), 1776 (C=O), 1506 (C-C) cm^{-1}; ^{1}H NMR ($CDCl_3$, 400 MHz,): $\delta = 7.54–7.52$ (2H, dd, $J = 8.8$, 1.5 Hz, H-13, H-9), 7.45–7.41 (2H, m, H-12, H-10), 7.33–7.29 (1H, m, H-11), 6.09 (1H, s, H-4), 2.52 (2H, q, $J = 7.6$ Hz, H-16), 2.32 (3H, s, H-7), 1.19 (3H, t, $J = 7.5$, H-17); ^{13}C NMR ($CDCl_3$, 100 MHz): $\delta = 169.7$ (C, C-14), 148.9 (C, C-3), 144.4 (C, C-5), 138.0 (C, C-8), 129.0 (CH, C-12, C-10), 127.1 (CH, C-11), 123.1 (CH, C-13, C-9), 95.8 (CH, C-4), 27.5 (CH_2, C-16), 14.5 (CH_3, C-7), 8.8 (CH_3, C-17); EIMS *m/z* (rel. int.) 230 $[M]^+$ (16), 175(22), 174(100), 129(18), 105(11), 77(75), 57(99), 51(14), 39(8), 29(35).

3-methyl-1-phenyl-1*H*-pyrazol-5-yl isobutyrate (4)

Dark yellow viscous oil (yield 90%); $C_{14}H_{16}N_2O_2$; IR (ATR diamond, cm^{-1}) 3066 (C-H aromatic), 2980 (C-H aliphatic), 1773 (C=O), 1506 (C-C) cm^{-1}; ^{1}H NMR ($CDCl_3$,

400 MHz,): $\delta = 7.54–7.50$ (2H, m, H-9, H-13), 7.45–7.40 (2H, m, H-10, H-12), 7.33–7.31 (1H, m, H-11), 6.08 (1H, s, H-4), 2.73 (1H, sept, $J = 7.0$ Hz, H-16), 2.32 (3H, s, H-7), 1.22 (6H, d, $J = 7.0$ Hz, H-17, H-18); ^{13}C NMR ($CDCl_3$, 100 MHz): $\delta = 172.4$ (C, C-14), 149.1 (C, C-3), 144.8 (C, C-5), 138.2 (C, C-8), 129.1 (CH, C-10, C-12), 127.3 (CH, C-11), 123.5 (CH, C-9, C-13), 95.8 (CH, C-4), 34.2 (CH, C-16), 18.8 (CH_3, C-17, C-18), 14.6 (CH_3, C-7); EIMS *m/z* (rel. int.) 244 $[M]^+$ (1), 174(5), 129(2), 117(1), 105(3), 91 (2), 77(38), 71(73), 51(11), 43(100), 41(9).

3-methyl-1-phenyl-1*H*-pyrazol-5-yl pentanoate (5)

Brown solid (yield 92%); $C_{15}H_{18}N_2O_2$; mp 108–110 °C; IR (ATR diamond, cm^{-1}) 3047 (C-H aromatic), 2914 (C-H aliphatic), 1709 (C=O) cm^{-1}; ^{1}H NMR ($CDCl_3$, 400 MHz,): $\delta = 7.55–7.48$ (2H, m, H-13, H-9), 7.46–7.37 (2H, m, H-12, H-10), 7.34–7.25 (1H, m, H-11), 6.08 (1H, s, H-4), 2.49 (2H, t, $J = 7.4$ Hz, H-16), 2.32 (3H, s, H-7), 1.70–1.55 (2H, m, H-17), 1.41–1.22 (2H, m, H-18), 0.89 (3H, t, $J = 7.1$ Hz, H-19); ^{13}C NMR ($CDCl_3$, 100 MHz): $\delta = 164.5$ (C, C-14), 144.4 (C, C-3), 139.9 (C, C-5), 133.4 (C, C-8), 124.6 (CH, C-10, C-12), 122.6 (CH, C-11), 118.8 (CH, C-9, C-13), 91.4 (CH, C-4), 29.2 (CH_2, C-16), 22.0 (CH_2, C-17), 17.5 (CH_2, C-18), 10.0 (CH_3, C-7), 9.2 (CH_3, C-19); EIMS *m/z* (rel. int.) 258 $[M]^+$ (1), 175(1), 174(10), 173(1), 129(1), 105(2), 85(42), 77(39), 57(100), 51(13), 41(36).

3-methyl-1-phenyl-1*H*-pyrazol-5-yl heptanoate (6)

Yellow viscous oil (yield 93%); $C_{17}H_{22}N_2O_2$; IR (ATR diamond, cm^{-1}) 3069 (C-H aromatic), 2928 (C-H aliphatic), 1782 (C=O), 1504 (C-C) cm^{-1}; ^{1}H NMR ($CDCl_3$, 400 MHz,): $\delta = 7.54–7.51$ (2H, m, H-9, H-13), 7.45–7.40 (2H, m, H-10, H-12), 7.33–7.29 (1H, m, H-11), 6.08 (1H, s, H-4), 2.49 (2H, t, $J = 7.4$ Hz, H-16), 2.32 (3H, s, H-7), 1.65 (2H, quint, $J = 7.4$ Hz, H-17), 1.33-1.23 (6H, m, H-18, H-19, H-20), 0.87 (3H, t, $J = 6.8$ Hz, H-21); ^{13}C NMR ($CDCl_3$, 100 MHz): $\delta = 169.2$ (C, C-14), 149.1 (C, C-3), 144.6 (C, C-5), 138.3 (C, C-8), 129.1 (CH, C-10, C-12), 127.3 (CH, C-11), 123.4 (CH, C-9, C-13), 95.9 (CH, C-4), 34.2 (CH_2, C-16), 31.5 (CH_2, C-17), 28.7 (CH_2, C-18), 24.7 (CH_2, C-19), 22.5 (CH_2, C-20), 14.6 (CH_3, C-7), 14.1 (CH_3, C-21); EIMS *m/z* (rel. int.) 286 $[M]^+$ (3), 174(100), 157(2), 145(3), 129(7), 113 (94), 105(8), 95(11), 85(86), 77(61), 57(48), 42(77), 39(8).

3-methyl-1-phenyl-1*H*-pyrazol-5-yl octanoate (7)

Orange-yellow liquid (yield 98%); $C_{18}H_{24}N_2O_2$; IR (ATR diamond, cm^{-1}) 3066 (C-H aromatic), 2926 (C-H aliphatic), 1784 (C=O), 1504 (C-C) cm^{-1}; ^{1}H NMR ($CDCl_3$, 400 MHz,): $\delta = 7.56–7.53$ (2H, m, H-9, H-13), 7.47–7.42 (2H, m, H-10, H-12), 7.35–7.31 (1H, m, H-11), 6.10 (1H, s, H-4), 2.51 (2H, t, $J = 7.4$ Hz, H-16), 2.34 (3H, s, H-7), 1.67 (2H, quint, $J = 7.4$ Hz, H-17), 1.33–1.27 (8H, m, H-18, H-19, H-20, H-21), 0.90 (3H, t, $J = 6.7$ Hz, H-22); ^{13}C NMR ($CDCl_3$, 100 MHz): $\delta = 169.0$ (C, C-14), 148.9 (C, C-3), 144.5 (C, C-5), 138.1 (C, C-8), 129.0 (CH, C-10, C-12), 127.1 (CH, C-11), 123.2 (CH, C-9, C-13), 95.8 (CH, C-4), 34.0 (CH_2, C-16), 31.5 (CH_2, C-19), 28.8 (CH_2, C-18), 28.8 (CH_2, C-20), 24.5 (CH_2, C-17), 22.5 (CH_2, C-21), 14.5 (CH_3, C-7), 14.0 (CH_3, C-22); EIMS *m/z* (rel. int.) 300 $[M]^+$ (2), 174(100), 157(2), 145(3), 127(84), 109(17), 105(9), 91 (4), 77(62), 67(16), 56(91), 43(36).

3-methyl-1-phenyl-1*H*-pyrazol-5-yl 2-propylpentanoate (8)

Yellow liquid (yield 92%); $C_{18}H_{24}N_2O_2$; IR (ATR diamond, cm^{-1}) 3050 (C-H aromatic), 2926 (C-H aliphatic), 1768 (C=O), 1506 (C-C) cm^{-1}; ^{1}H NMR ($CDCl_3$, 400 MHz,): $\delta = 7.55–7.53$ (2H, m, H-9, H-13), 7.46–7.42 (2H, m, H-10, H-12), 7.35–7.31 (1H, m, H-11), 6.08 (1H, s, H-4), 2.56 (1H, tt, $J = 8.8$, 5.4 Hz, H-16), 2.34 (3H, s, H-7), 1.70–1.60 (2H, m, H-20), 1.53–1.46 (2H, m, H-17), 1.27 (4H, sext, $J = 7.4$ Hz, H-18, H-21), 0.88 (6H, t, $J = 7.3$ Hz, H-19, H-22); ^{13}C NMR ($CDCl_3$, 100 MHz): $\delta = 171.7$ (C, C-14), 148.9 (C, C-3), 144.6 (C, C-5), 138.0 (C, C-8), 128.9 (CH, C-10, C-12), 127.2 (CH, C-11), 123.7 (CH, C-9, C-13), 95.6 (CH, C-4), 45.3 (CH, C-16), 34.2 (CH_2, C-17, C-20), 20.5 (CH_2, C-18, C-21), 14.5 (CH_3, C-7), 13.9 (CH_3, C-19, C-22); EIMS *m/z* (rel. int.) 300 $[M]^+$ (1), 174(1), 127(5), 99 (10), 77(13), 57(100), 43(8).

3-methyl-1-phenyl-1*H*-pyrazol-5-yl benzoate (9)

Cream color powder (yield 99%); $C_{17}H_{14}N_2O_2$; mp 118 °C; IR (ATR diamond, cm^{-1}) 3069 (C-H aromatic), 1755 (C=O), 1504 (C-C) cm^{-1}; ^{1}H NMR ($CDCl_3$, 400 MHz,): $\delta =$ 8.01–7.96 (2H, m, H-17, H-21), 7.59–7.48 (3H, m, H-9, H-13, H-19), 7.43–7.29 (4H, m, H-10, H-12, H-18, H-20), 7.25–7.17 (1H, m, H-11), 6.19 (1H, s, H-4), 2.28 (3H, s, H-7); ^{13}C NMR ($CDCl_3$, 100 MHz): $\delta = 161.9$ (C, C-14), 149.1 (C, C-3), 144.5 (C, C-5), 138.1 (C, C-8), 134.4 (C, C-16), 130.5 (CH, C-19), 129.1 (CH, C-10, C-12), 128.9 (CH, C-18, C-20), 127.9 (CH, C-11) 127.2 (CH, C-17, C-21), 123.2 (CH, C-9, C-13), 95.9 (CH, C-4), 14.7 (CH_3, C-7); EIMS *m/z* (rel. int.) 278 $[M]^+$ (1), 106(8), 105(100), 77(62), 51(15).

3-methyl-1-phenyl-1*H*-pyrazol-5-yl 4-methylbenzoate (10)

Cream color crystals (yield 99%); $C_{18}H_{16}N_2O_2$; mp 105–106 °C; IR (ATR diamond, cm^{-1}) 3058 (C-H aromatic), 1752 (C=O), 1504 (C-C) cm^{-1}; ^{1}H NMR ($CDCl_3$, 400 MHz,): $\delta = 7.96–7.90$ (2H, m, H-17, H-21), 7.61–7.54 (2H, m, H-9, H-13), 7.44–7.22 (5H, m, H-10, H-11, H-12, H-18, H-20), 6.24 (1H, s, H-4), 2.40 (3H, s, H-22), 2.34 (3H,

s, H-7); ^{13}C NMR ($CDCl_3$, 100 MHz): $\delta = 162.0$ (C, C-14), 149.2 (C, C-3), 145.5 (C, C-5), 144.7 (C, C-19), 138.1 (C, C-8), 130.5 (CH, C-10, C-12), 129.6 (CH, C-18, C-20), 129.2 (CH, C-17, C-21), 127.3 (CH, C-11), 125.2 (C, C-16), 123.3 (CH, C-9, C-13), 96.0 (CH, C-4), 21.9 (CH_3, C-22), 14.6 (CH_3, C-7); EIMS *m/z* (rel. int.) 292 $[M]^+$ (1), 119 (100), 91(38), 77(20), 65(15), 51(7).

3-methyl-1-phenyl-1*H*-pyrazol-5-yl 2-methylbenzoate (11)

Cream color powder (yield 95%); $C_{18}H_{16}N_2O_2$; mp 104 °C; IR (ATR diamond, cm^{-1}) 3066 (C-H aromatic), 2923 (C-H aliphatic), 1744 (C=O), 1506 (C-C) cm^{-1}; ^{1}H NMR ($CDCl_3$, 400 MHz,): $\delta = 8.02$ (1H, dd, $J = 7.8$, 1.4 Hz, H-17), 7.62 (2H, dd, $J = 8.7$, 1.4 Hz, H-9, H-13), 7.49 (1H, ddd, $J = 7.5$, 7.5, 1.5 Hz, H-19), 7.46–7.41 (2H, m, H-10, H-12), 7.35–7.27 (3H, m, H-11, H-18, H-20), 6.26 (1H, s, H-4), 2.61 (3H, s, H-22), 2.40 (3H, s, H-7); ^{13}C NMR ($CDCl_3$, 100 MHz): $\delta = 162.2$ (C, C-14), 149.0 (C, C-3), 144.7 (C, C-5), 142.2 (C, C-21), 138.2 (C, C-8), 133.4 (CH, C-19), 132.1 (CH, C-20), 131.1 (CH, C-17), 129.0 (CH, C-10, C-12), 127.2 (CH, C-11), 126.8 (C, C-16), 126.1 (CH, C-18), 123.4 (CH, C-9, C-13), 95.9 (CH, C-4), 21.8 (CH_3, C-22). 14.5 (CH_3, C-7); EIMS *m/z* (rel. int.) 292 $[M]^+$ (1), 173(2), 120(18), 118(100), 106(2), 91(75), 77(31), 65(27), 51(9), 39(8).

3-methyl-1-phenyl-1*H*-pyrazol-5-yl 2-(naphthalen-1-yl) acetate (12)

Yellow viscous oil (yield 70%); $C_{22}H_{18}N_2O_2$; IR (ATR diamond, cm^{-1}) 3031 (C-H aromatic), 2920 (C-H aliphatic), 1714 (C=O) cm^{-1}; ^{1}H NMR ($CDCl_3$, 400 MHz,): $\delta =$ 7.93–7.89 (2H, m, H-20, H-26), 7.87 (1H, d, $J = 8.0$ Hz, H-23), 7.55–7.48 (2H, m, H-10, H-12), 7.46–7.40 (2H, m, H-24, H-25), 7.26–7.24 (2H, m, H-9, H-13), 7.22–7.18 (3H, m, H-11, H-21, H-22), 6.16 (1H, s, H-4), 4.26 (2H, s, H-16), 2.33 (3H, s, H-7); ^{13}C NMR ($CDCl_3$, 100 MHz): $\delta =$ 166.5 (C, C-14), 148.8 (C, C-3), 144.3 (C, C-5), 137.8 (C, C-8), 133.9 (C, C-19), 132.0 (C, C-18), 128.9 (C, C-17), 128.8 (CH, C-10, C-12), 128.7 (CH, C-20), 128.6 (CH, C-26), 128.5 (CH, C-24), 126.8 (CH, C-22), 126.8 (CH, C-11), 126.1 (CH, C-21), 125.5 (CH, C-25), 123.3 (CH, C-23), 122.8 (CH, C-9, C-13), 95.7 (CH, C-4), 39.0 (CH_2, C-16), 14.5 (CH_3, C-7); EIMS *m/z* (rel. int.) 342 $[M]^+$ (2), 174 (3), 168(28), 141(100), 115(23), 105(2), 91(2), 77(46), 63 (5), 51(13), 40(7).

3-methyl-1-phenyl-1*H*-pyrazol-5-yl diphenylcarbamate (13)

Cream color crystals (yield 98%); $C_{23}H_{19}N_3O_2$; mp 95–96 °C; IR (ATR diamond, cm^{-1}) 3061 (C-H aromatic), 1747 (C=O), 1504 (C-C), 1303 (C-N) cm^{-1}; ^{1}H NMR ($CDCl_3$, 400 MHz,): $\delta = 7.40$–7.32 (5H, m, H-9, H-10, H-11, H-12, H-13), 7.29–7.20 (10H. m, H-19, H-20, H-21, H-22, H-23, H-24, H-25, H-26, H-27, H-28), 6.23 (1H, s, H-4), 2.34 (3H, s, H-7); ^{13}C NMR ($CDCl_3$, 100 MHz): $\delta =$ 149.7 (C, C-14), 148.8 (C, C-3), 144.9 (C, C-5), 141.4 (C, C-17, C-18), 137.9 (C, C-8), 129.3 (CH, C-10, C-12), 128.8 (CH, C-20, C-22, C-25, C-27), 127.1 (CH, C-11, C21, C-26), 126.6 (CH, C-9, C-13), 122.8 (CH, C-19, C-23, C-24, C-28), 95.1 (CH, C-4), 14.5 (CH_3, C-7); EIMS *m/z* (rel. int.) 369 $[M]^+$ (1), 196(100), 168(53), 167(27), 139(1), 115(2), 93(8), 77(53), 65(4), 51(12), 39(3).

3-methyl-1-phenyl-1*H*-pyrazol-5-yl cinnamate (14)

Cream color powder (yield 93%); $C_{19}H_{16}N_2O_2$; mp 107–108 °C; IR (ATR diamond, cm^{-1}) 2920 (C-H aliphatic), 1747 (C=O), 1504 (C-C) cm^{-1}; ^{1}H NMR ($CDCl_3$, 400 MHz,): $\delta = 7.83$ (1H, d, $J = 16$ Hz, H-17), 7.60–7.57 (2H, m, H-9, H-13), 7.56–7.53 (2H, m, H-19, H-23), 7.47–7.39 (5H, m, H-10, H-12, H-20, H-21, H-22), 7.34–7.29 (1H, m, H-11), 6.51 (1H, d, $J = 15.9$ Hz, H-16), 6.20 (1H, s, H-4), 2.35 (3H, s, H-7); ^{13}C NMR ($CDCl_3$, 100 MHz): $\delta = 162.1$ (C, C-14), 149.0 (C, C-3), 148.5 (CH, C-17), 144.5 (C, C-5), 138.2 (C, C-8), 133.7 (C, C-18), 131.3 (CH, C-21), 129.1 (CH, C-10, C-12), 129.1 (CH, C-20, C-22), 128.5 (CH, C-19, C-23), 127.1 (CH, C-11), 123.1 (CH, C-9, C-13), 115.4 (CH, C-16), 95.8 (CH, C-4), 14.6 (CH_3, C-7); EIMS *m/z* (rel. int.) 304 $[M]^+$ (1), 173(3), 131(61), 104(4), 103(45), 77(100), 51 (37).

3-methyl-1-phenyl-1*H*-pyrazol-5-yl 5-phenylpentanoate (15)

Light yellow viscous oil (yield 90%); $C_{21}H_{22}N_2O_2$; IR (ATR diamond, cm^{-1}) 3023 (C-H aromatic), 2928 (C-H aliphatic), 1779 (C=O), 1504 (C-C) cm^{-1}; ^{1}H NMR ($CDCl_3$, 400 MHz,): $\delta = 7.52$–7.49 (2H, m, H-9, H-13), 7.42–7.37 (2H, m, H-10, H-12), 7.31–7.26 (3H, m, H-22, H-23, H-24), 7.21–7.16 (1H, m, H-11), 7.13 (2H, dd, $J = 8.2$, 1.6 Hz, H-21, H-25), 6.07 (1H, s, H-4), 2.60 (2H, t, $J = 7.5$ Hz, H-16), 2.52 (2H, t, $J = 7.0$ Hz, H-19), 2.32 (3H, s, H-7), 1.74–1.59 (4H, m, H-17, H-18); ^{13}C NMR ($CDCl_3$, 100 MHz): $\delta =$ 169.0 (C, C-14), 149.1 (C, C-3), 144.6 (C, C-5), 141.8 (C, C-8), 129.2 (CH, C-10, C-12), 128.5 (CH, C-22, C-24), 128.5 (CH, C-21, C-25), 127.3 (CH, C-23), 126.1 (CH, C-11), 123.4 (CH, C-9, C-13), 95.9 (CH, C-4), 35.6 (CH_2, C-16), 34.1 (CH_2, C-19), 30.7 (CH_2, C-17), 24.3 (CH_2, C-18), 14.6 (CH_3, C-7); EIMS *m/z* (rel. int.) 334 $[M]^+$ (1), 175(9), 174(56), 143(3), 133(3), 117(76), 104(5), 91(100), 77(40), 65(8), 51(5), 39(4).

DPPH assay antioxidant evaluation

The radical-scavenging activity was analyzed based on the methodology by Salazar-Aranda [56] with slight modifications. The products were dissolved with methanol and different concentrations were obtained by serial dilutions. An aliquot of 0.5 mL from each dilution was mixed with 0.5 mL of a DPPH methanolic solution (prepared at a concentration 7.5 mg/250 mL). The mixtures were incubated for 30 min in the dark at room temperature. After this time, the spectrophotometric measurement of the mixtures was performed at 517 nm, employing methanol as a blank. The radical-scavenging activity was calculated as the percentage of DPPH discoloration with the formula:

$$\text{DPPH}\ (\%) = \left(1 - \frac{B}{A}\right) \times 100,$$

where the value of a DPPH solution as control is represented by A and the sample by B. All determinations were performed in triplicate. The DPPH discoloration was plotted against the concentration of each dilution, and by interpolation employing a linear regression analysis, the concentration needed to decrease the absorbance of DPPH by 50% (EC_{50}) was obtained. As a reference compound, quercetin was employed.

ABTS assay antioxidant evaluation

The ABTS radical cation ($ABTS^{\cdot+}$) scavenging assay was analyzed based on reported methodologies [57, 58] with slight modifications. An aqueous solution of ABTS was prepared at a 7 mM concentration. The radical cation $ABTS^{\cdot+}$ was produced by the reaction between the ABTS solution with a 2.45 mM potassium persulfate solution; the mixture was kept at room temperature in the dark for 16–18 h before use. Then 150 µL of the $ABTS^{\cdot+}$ solution was diluted with methanol to obtain an absorbance 0.7 ± 0.02 as an initial absorbance, at a wavelength of 754 nm. A volume of 980 µL from this solution was mixed with 20 µL of the different concentrations prepared of the samples. The mixture was stirred and incubated for 7 min at room temperature, before reading the final absorbance. The percentage of inhibition was calculated using the formula:

$$\%\ \text{of inhibition} = \left(\frac{A_1 - A_2}{A_1}\right) \times 100,$$

where the initial absorbance of the $ABTS^{\cdot+}$ solution is A_1 and the final absorbance in the presence of the sample is A_2. All determinations were performed in triplicate. For each compound, the concentration of each dilution was plotted against the percentage of inhibition, and the EC_{50} value was obtained by interpolation from a linear regression analysis. As a reference compound, quercetin was employed [59].

AChE inhibitory activity

AChE inhibitory activity was determined employing a previously reported methodology [15] with slight modifications. In a 96-well plate, 75 µL of a 50 mM Trizma-HCl buffer (pH = 8) was added with 75 µL of a solution of the synthesized compound to analyze, obtaining at the end a final concentration of 150 µg/mL (0.15% for dimethyl sulfoxide). Then, to each well, 25 µL of a buffer solution of 15 mM acetylthiocoline chloride was added, along with 125 µL of a 3 mM buffer solution of Ellman's reagent (DTNB), with final concentrations of 1.25 mM for both. Employing a microplate reader every 45 s, the absorbance was measured at a wavelength of 405 nm, three consecutive times. Afterwards, to each well 25 µL of a 2 U/mL AChE in buffer solution was added, enriched with bovine serum albumin (0.1 mg/mL), with a final concentration of the enzyme at 0.15 U/mL. Five consecutive lectures were taken every 45 s. Six wells from each plate had no tested compound in them in order to serve as the control for the enzyme 100% activity. To correct the substrate's spontaneous hydrolysis, the absorbance from before the enzyme addition was subtracted from the absorbance obtained after. The percentage of inhibition was calculated using the formula:

$$\%\ \text{of inhibition} = 1 - \left(\frac{A_{\text{sample}}}{A_{\text{control}}}\right) \times 100,$$

where the absorbance difference between time 0 and 225 s in the presence of the compound to test is represented by A_{Sample} and the corresponding absorbance difference of the 100% AChE activity control is represented by A_{Control}. All experiments were performed in triplicate. As a positive control, galantamine was employed [60].

Molecular docking

The methodology was based on a previous work [61]. Molecular models were generated for the analyzed products through their SMILES strings with the use of UCSF Chimera [62]. These models were energy minimized employing Chimera default conditions with Antechamber parameters [63]. With AutoDock Tools 1.5.6 [64] were defined the rotatable bonds and the atomic charges for each model. The crystallographic structure of the AChE receptor (PDB ID: 1EVE) was retrieved from Protein Data Bank (http://www.rcsb.org/), which was prepared with AutoDock Tools removing the co-crystalized ligand (donepezil) along with the water molecules, hydrogen addition, and Gasteiger charge calculation. For the docking analysis, AutoDock Vina was employed [65], with a grid of 28 × 28 × 28 Å, with center coordinates at $x = 3.11011$, $y = 66.7013$, and $z = 63.9449$. For each

ligand, ten poses were generated with an exhaustiveness of eight, making the docking runs by triplicate. The visualization and analysis of the docked poses was made with UCSF Chimera.

ADME calculations

The drug-likeness prediction of the synthesized compounds was made by obtaining their pharmacokinetic and physicochemical properties using the SwissADME web server [66].

Acknowledgements We gratefully acknowledge the Facultad de Ciencias Químicas e Ingeniería, Universidad Autónoma de Baja California for the financing given for the realization of this project. Additionally, to the Consejo Nacional de Ciencia y Tecnología (CONACYT) for ITT NMR facilities (Grant INFR-2011-3-173395).

Compliance with ethical standards

Conflict of interest The authors declare that they have no conflict of interest.

Publisher's note Springer Nature remains neutral with regard to jurisdictional claims in published maps and institutional affiliations.

References

1. Mangialasche F, Solomon A, Winblad B, Mecocci P, Kivipelto M. Alzheimer's disease: clinical trials and drug development. Lancet Neurol. 2010;9:702–16. https://doi.org/10.1016/S1474-4422(10)70119-8.
2. Lin HQ, Ho MT, Lau LS, Wong KK, Shaw PC, Wan DCC. Anti-acetylcholinesterase activities of traditional Chinese medicine for treating Alzheimer's disease. Chem Biol Interact. 2008;175:352–4. https://doi.org/10.1016/j.cbi.2008.05.030.
3. Calissano P, Matrone C, Amadoro G. Apoptosis and in vitro Alzheimer's disease neuronal models. Commun Integr Biol. 2009;2:163–9. https://doi.org/10.4161/cib.7704.
4. Shah RS, Lee H-G, Xiongwei Z, Perry G, Smith MA, Castellani RJ. Current approaches in the treatment of Alzheimer's disease. Biomed Pharmacother. 2008;62:199–207. https://doi.org/10.1016/j.biopha.2008.02.005.
5. Butterfield DA, Castegna A, Pocernich CB, Drake J, Scapagnini G, Calabrese V. Nutritional approaches to combat oxidative stress in Alzheimer's disease. J Nutr Biochem. 2002;13:444–61. https://doi.org/10.1016/s0955-2863(02)00205-x.
6. Christen Y. Oxidative stress and Alzheimer disease. Am J Clin Nutr. 2000;71:621S–9S. https://doi.org/10.1093/ajcn/71.2.621s.
7. Birben E, Sahiner UM, Sackesen C, Erzurum S, Kalayci O. Oxidative stress and antioxidant defense. World Allergy Organ J 2012;5:9–19. https://doi.org/10.1097/WOX.0b013e3182439613.
8. Smith MA, Rottkamp CA, Nunomura A, Raina AK, Perry G. Oxidative stress in Alzheimer disease. Biochim Biophys Acta. 2000;1502:139–44. https://doi.org/10.1016/s0925-4439(00)00040-5.
9. Roberts CK, Sindhu KK. Oxidative stress and metabolic syndrome. Life Sci. 2009;84:705–12. https://doi.org/10.1016/j.lfs.2009.02.026.
10. Huang W-J, Zhang X, Chen W-W. Role of oxidative stress in Alzheimer's disease. Biomed Rep. 2016;4:519–22. https://doi.org/10.3892/br.2016.630.
11. Chauhan V, Chauhan A. Oxidative stress in Alzheimer's disease. Pathophysiology 2006;13:195–208. https://doi.org/10.1016/j.pathophys.2006.05.004.
12. Guan Z-Z. Cross-talk between oxidative stress and modifications of cholinergic and glutaminergic receptors in the pathogenesis of Alzheimer's disease. Acta Pharmacol Sin. 2008;29:773–80. https://doi.org/10.1111/j.1745-7254.2008.00819.x.
13. Liu Z, Qin G, Mana L, Dong Y, Huang S, Wang Y, et al. GAPT regulates cholinergic dysfunction and oxidative stress in the brains of learning and memory impairment mice induced by scopolamine. Brain Behav. 2020;10:e01602 https://doi.org/10.1002/brb3.1602.
14. Singh M, Kaur M, Kukreja H, Chugh R, Silakari O, Singh D. Acetylcholinesterase inhibitors as Alzheimer therapy: from nerve toxins to neuroprotection. Eur J Med Chem. 2013;70:165–88. https://doi.org/10.1016/j.ejmech.2013.09.050.
15. Adewusi EA, Moodley N, Steenkamp V. Antioxidant and acetylcholinesterase inhibitory activity of selected southern African medicinal plants. S Afr J Bot. 2011;77:638–44. https://doi.org/10.1016/j.sajb.2010.12.009.
16. Holzgrabe U, Kapková P, Alptüzün V, Scheiber J, Kugelmann E. Targeting acetylcholinesterase to treat neurodegeneration. Expert Opin Ther Targets. 2007;11:161–79. https://doi.org/10.1517/14728222.11.2.161.
17. Zambrano P, Suwalsky M, Jemiola-Rzeminska M, Strzalka K, Sepúlveda B, Gallardo MJ, et al. The acetylcholinesterase (AChE) inhibitor and anti-Alzheimer drug donepezil interacts with human erythrocytes. Biochim Biophys Acta Biomembr. 2019;1861:1078–85. https://doi.org/10.1016/j.bbamem.2019.03.014.
18. Pal S, Mareddy J, Devi NS. High speed synthesis of pyrazolones using microwave-assisted neat reaction technology. J Braz Chem Soc. 2008;19:1207–14. https://doi.org/10.1590/S0103-50532008000600023.
19. Schiel MA, Chopa AB, Silbestri GF, Alvarez MB, Lista AG, Domini CE. Use of ultrasound in the synthesis of heterocycles of medicinal interest. In: Brahmachari G, editor. Green synthetic approaches for biologically relevant heterocycles. Boston: Elsevier; 2015. p. 571–601.
20. Gautam S, Rani S, Aldossary SA, Saeedan AS, Ansari MN, Kaithwas G. Effects of phenidone (DuCLOX-2/5 inhibitor) against *N*-methyl-*N*-nitrosurea induced mammary gland carcinoma in albino rats. Toxicol Appl Pharm. 2018;351:57–63. https://doi.org/10.1016/j.taap.2018.04.019.
21. Russo S, Filgueira, de Azevedo W. Computational analysis of dipyrone metabolite 4-aminoantipyrine as a cannabinoid receptor 1 agonist. Curr Med Chem. 2020;27:4741–9. https://doi.org/10.2174/0929867326666190906155339.
22. Higashi Y, Jitsuiki D, Chayama K, Yoshizumi M. Edaravone (3-methyl-1-phenyl-2-pyrazolin-5-one), a novel free radical scavenger, for treatment of cardiovascular diseases. Recent Pat Cardiovasc Drug Disco. 2006;1:85–93. https://doi.org/10.2174/157489006775244191.
23. Watanabe T, Tahara M, Todo S. The novel antioxidant edaravone: from bench to bedside. Cardiovasc Ther. 2008;26:101–14. https://doi.org/10.1111/j.1527-3466.2008.00041.x.
24. Marković V, Erić S, Juranić ZD, Stanojković T, Joksović L, Ranković B, et al. Synthesis, antitumor activity and QSAR studies of some 4-aminomethylidene derivatives of edaravone. Bioorg Chem. 2011;39:18–27. https://doi.org/10.1016/j.bioorg.2010.10.003.
25. Fan X, Zhang X, Zhou L, Keith KA, Kern ER, Torrence PF. A pyrimidine-pyrazolone nucleoside chimera with potent in vitro anti-orthopoxvirus activity. Bioorg Med Chem Lett. 2006;16:3224–8. https://doi.org/10.1016/j.bmcl.2006.03.043.
26. Alzoubi KH, Al Mosabih HS, Mahasneh AF. The protective effect of edaravone on memory impairment induced by chronic sleep

deprivation. Psychiatry Res. 2019;281:112577 https://doi.org/10.1016/j.psychres.2019.112577.
27. Li K, Chen C, Huang Q, Zhang Y, Yao S. Efficacy of edaravone combined with rt-PA in treatment of acute cerebral infarction and the relation with inflammatory response and oxidative stress. Lat Am J Pharm. 2020;39:511–7.
28. Wang B, Lin W. Edaravone protects against pancreatic and intestinal injury after acute pancreatitis via nuclear factor-κB signaling in mice. Biol Pharm Bull. 2020;43:509–15. https://doi.org/10.1248/bpb.b19-00944.
29. Gao Y-K, Gui C-J, Xin W-Q, Hu D, Yang X-Y. Assessment of mild hypothermia combined with edaravone for the treatment of severe craniocerebral injury. Trop J Pharm Res. 2019;18:2557–62. https://doi.org/10.4314/tjpr.v18i12.14.
30. Spasić S, Nikolić-Kokić A, Miletić S, Oreščanin-Dušić Z, Spasić MB, Blagojević D, et al. Edaravone may prevent ferroptosis in ALS. Curr Drug Targets. 2020;21:776–80. https://doi.org/10.2174/1389450121666200220123305.
31. Pan Y, Li W, Feng Y, Xu J, Cao H. Edaravone attenuates experimental asthma in mice through induction of HO-1 and the Keap1/Nrf2 pathway. Exp Ther Med. 2020;19:1407–16. https://doi.org/10.3892/etm.2019.8351.
32. Jensen BS. The synthesis of 1-phenyl-3-methyl-4-acyl-pyrazolones-5. Acta Chem Scand. 1959;13:1668–70. https://doi.org/10.3891/acta.chem.scand.13-1668.
33. Zamorano S, Camus J. Síntesis y caracterización RMN 1D y 2D de derivados sulfurados de la 1-fenil-3-metil-2-pirazolín-5-ona y su potencial capacidad ligante. Rev Soc Quím Perú. 2015;81:24–32.
34. Holzer W, Guo C, Schalle K. 3-Methyl-1-phenyl-1*H*-pyrazol-5-yl 2-bromo-3-furan-carboxylate. Molbank 2009;2009:M603 https://doi.org/10.3390/M603.
35. Xie C, Lu Z, Zhou W, Han J, Pan Y. A facile organocatalyzed Michael addition of pyrazolines to α,β-unsaturated carbonyl compounds. Tetrahedron Lett. 2012;53:6650–3. https://doi.org/10.1016/j.tetlet.2012.09.096.
36. Levin A. Orally bioavailable prodrugs of edaravone with altered pharmacokinetic properties and methods of use thereof. Patent no. WO 2019/213335 A1. 2019.
37. Maruoka H, Yamagata K, Okabe F, Tomioka Y. Synthesis of 1-acyl-1,2-dihydro-3*H*-pyrazol-3-ones via Lewis acid-mediated rearrangement of 3-acyloxypyrazoles. J Heterocycl Chem. 2006;43:859–65. https://doi.org/10.1002/jhet.5570430408.
38. Bai Y, Lu J, Gan H, Wang Z. Rapid microwave-enhanced synthesis of 1-phenyl-3-methyl-5-acyloxypyrazoles under solvent-free conditions. Synth Commun. 2002;32:2549–53. https://doi.org/10.1081/SCC-120005938.
39. Terebenina A, Todorova O, Simova S, Borisov G. Reaction of 3-methyl-1-phenyl-5-pyrazolone with some unsaturated aliphatic carboxylic acid chlorides. Izv Khim. 1989;22:236–45.
40. Borges RS, Queiroz AN, Mendes APS, Araújo SC, França LCS, Franco ECS, et al. Density functional theory (DTF) study of edaravone derivatives as antioxidants. Int J Mol Sci. 2012;13:7594–606. https://doi.org/10.3390/ijms13067594.
41. Polkam N, Ramaswamy VR, Rayam P, Allaka TR, Anantaraju HS, Dharmarajan S, et al. Synthesis, molecular properties prediction and anticancer, antioxidant evaluation of new edaravone derivatives. Bioorg Med Chem Lett. 2016;26:2562–8. https://doi.org/10.1016/j.bmcl.2016.03.024.
42. Minelli C, Laudadio E, Galeazzi R, Rusciano D, Armeni T, Stipa P, et al. Synthesis, characterization and antioxidant properties of a new lipophilic derivative of edaravone. Antioxidants 2019;8:258 https://doi.org/10.3390/antiox8080258.
43. Nakagawa H, Ohyama R, Kimata A, Suzuki T, Miyata N. Hydroxyl radical scavenging by edaravone derivatives: efficient scavenging by 3-methyl-1-(pyridin-2-yl)-5-pyrazolone with an intramolecular base. Bioorg Med Chem Lett. 2006;16:5939–42. https://doi.org/10.1016/j.bmcl.2006.09.005.
44. Ilyasov IR, Beloborodov VL, Selivanova IA, Terekhov RP. ABTS/PP decolorization assay of antioxidant capacity reaction pathways. Int J Mol Sci. 2020;21:1131 https://doi.org/10.3390/ijms21031131.
45. Jiao SS, Yao XQ, Liu YH, Wang QH, Zeng F, Lu JJ, et al. Edaravone alleviates Alzheimer's disease-type pathologies and cognitive deficits. Proc Natl Acad Sci USA. 2015;112:5225–30. https://doi.org/10.1073/pnas.1422998112.
46. Zondagh LS, Malan SF, Joubert J. Design, synthesis and biological evaluation of edaravone derivatives bearing the *N*-benzyl pyridinium moiety as multifunctional anti-Alzheimer's agents. J Enzym Inhib Med Chem. 2020;35:1596–605. https://doi.org/10.1080/14756366.2020.1801673.
47. Yang R, Wang Q, Li F, Li J, Liu X. Edaravone injection ameliorates cognitive deficits in rat model of Alzheimer's disease. Neurol Sci. 2015;36:2067–72. https://doi.org/10.1007/s10072-015-2314-y.
48. Jangra A, Kwatra M, Singh T, Pant R, Kushwah P, Ahmed S, et al. Edaravone alleviates cisplatin-induced neurobehavioral deficits via modulation of oxidative stress and inflammatory mediators in the rat hippocampus. Eur J Pharmacol. 2016;791:51–61. https://doi.org/10.1016/j.ejphar.2016.08.003.
49. Chiou S-Y, Huang C-F, Hwang M-T, Lin G. Comparison of active sites of butyrylcholinesterase and acetylcholinesterase based on inhibition by geometric isomers of benzene-di-*N*-substituted carbamates. J Biochem Mol Toxicol. 2009;23:303–8. https://doi.org/10.1002/jbt.20286.
50. Srivastava P, Tripathi PN, Sharma P, Rai SN, Singh SP, Srivastava RK, et al. Design and development of some phenyl benzoxazole derivatives as a potent acetylcholinesterase inhibitor with antioxidant property to enhance learning and memory. Eur J Med Chem. 2019;163:116–35. https://doi.org/10.1016/j.ejmech.2018.11.049.
51. Sarikaya G, Çoban G, Parlar S, Tarikogullari AH, Armagan G, Erdoğan MA, et al. Multifunctional cholinesterase inhibitors for Alzheimer's disease: synthesis, biological evaluations, and docking studies of *o*/*p*-propoxyphenylsubstituted-1*H*-benzimidazole derivatives. Arch Pharm Chem Life Sci. 2018;351:e1800076 https://doi.org/10.1002/ardp.201800076.
52. Kryger G, Silman I, Sussman JL. Structure of acetylcholinesterase complexed with E2020 (Aricept®): Implications for the design of new anti-Alzheimer drugs. Structure. 1999;7:297–307. https://doi.org/10.1016/s0969-2126(99)80040-9.
53. Bartolucci C, Perola E, Pilger C, Fels G, Lamba D. Three-dimensional structure of a complex of galanthamine (Nivalin®) with acetylcholinesterase from *Torpedo californica*: Implication for the design of new anti-Alzheimer drugs. Proteins 2001;42:182–91. https://doi.org/10.1002/1097-0134(20010201)42:2<182::aid-prot50>3.0.co;2-1.
54. Lipinski CA, Lombardo F, Dominy BW, Feeney PJ. Experimental and computational approaches to estimate solubility and permeability in drug discovery and development settings. Adv Drug Deliv Rev. 2001;46:3–26. https://doi.org/10.1016/s0169-409x(00)00129-0.
55. Jakki SL, Senthil V, Yasam VR, Chandrasekar MJN, Vijayaraghavan C. The blood brain barrier and its role in Alzheimer's therapy: an over-view. Curr Drug Targets. 2018;19:155–69. https://doi.org/10.2174/1389450118666170612100750.
56. Salazar-Aranda R, Granados-Guzmán G, Pérez-Meseguer J, González GM, Waksman, de Torres N. Activity of polyphenolic compounds against Candida glabrata. Molecules 2015;20:17903–12. https://doi.org/10.3390/molecules201017903.
57. Re R, Pellegrini N, Proteggente A, Pannala A, Yang M, Rice-Evans C. Antioxidant activity applying an improved ABTS radical

cation decolorization assay. Free Radic Biol Med. 1999;26:1231–7. https://doi.org/10.1016/s0891-5849(98)00315-3.
58. Kuskoski EM, Asuero AG, Troncoso AM, Mancini-Filho J, Fett R. Aplicación de diversos métodos químicos para determinar actividad antioxidante en pulpa de frutos. Food Sci Technol. 2005;25:726–32. https://doi.org/10.1590/S0101-20612005000400016.
59. Noriega-Iribe E, Díaz-Rubio L, Estolano-Cobián A, Barajas-Carrillo VW, Padrón JM, Salazar-Aranda R, et al. In vitro and in silico screening of 2,4,5-trisubstituted imidazole derivatives as potential xanthine oxidase and acetylcholinesterase inhibitors, antioxidant, and antiproliferative agents. Appl Sci. 2020;10:2889 https://doi.org/10.3390/app10082889.
60. Díaz-Rubio L, Hernández-Martínez R, Estolano-Cobián A, Chávez-Velasco D, Salazar-Aranda R, Waksman de Torres N, et al. Synthesis, biological evaluation and docking studies of chalcone and flavone analogs as antioxidants and acetylcholinesterase inhibitors. Appl Sci. 2019;9:410 https://doi.org/10.3390/app9030410.
61. Galindo-Hernández O, Córdova-Guerrero I, Díaz-Rubio LJ, Pulido-Capiz A, Díaz-Villanueva JF, Castañeda-Sánchez CY, et al. Protein translation associated to PERK arm is a new target for regulation of metainflammation: a connection with hepatocyte cholesterol. J Cell Biochem. 2019;120:4158–71. https://doi.org/10.1002/jcb.27701.
62. Pettersen EF, Goddard TD, Huang CC, Couch GS, Greenblatt DM, Meng EC, et al. UCSF Chimera–a visualization system for exploratory research and analysis. J Comput Chem. 2004;25:1605–12. https://doi.org/10.1002/jcc.20084.
63. Wang J, Wang W, Kollman PA, Case DA. Automatic atom type and bond type perception in molecular mechanical calculations. J Mol Graph Model. 2006;25:247–60. https://doi.org/10.1016/j.jmgm.2005.12.005.
64. Sanner MF. Python: A programming language for software integration and development. J Mol Graph Model. 1999;17:57–61. https://doi.org/10.1016/S1093-3263(99)99999-0
65. Trott A, Olson AJ. AutoDock Vina: Improving the speed and accuracy of docking with a new scoring function, efficient optimization, and multithreading. J Comput Chem. 2010;31:455–61. https://doi.org/10.1002/jcc.21334.
66. Daina A, Michielin O, Zoete V. SwissADME: a free web tool to evaluate pharmacokinetics, drug-likeness and medicinal chemistry friendliness of small molecules. Sci Rep. 2017;7:42707 https://doi.org/10.1038/srep42717.
67. Ali J, Camilleri P, Brown MB, Hutt AJ, Kirton SB. Revisiting the general solubility equation: in silico prediction of aqueous solubility incorporating the effect of topographical polar surface area. J Chem Inf Model. 2012;52:420–8. https://doi.org/10.1021/ci200387c.